

# Oscillatory dynamics induced in polyelectrolyte gels by a non-oscillatory reaction: A model

J. Boissonade<sup>a</sup>

Université de Bordeaux and CNRS, Centre de Recherche Paul Pascal, 115 av. Schweitzer, F-33600 Pessac, France

Received 22 September 2008

Published online: 19 February 2009 – © EDP Sciences / Società Italiana di Fisica / Springer-Verlag 2009

**Abstract.** We develop a general model and the associated numerical algorithm to compute the swelling dynamics of chemo-responsive polyelectrolyte gels immersed in a reactive ionic solution kept at a non-equilibrium stationary state by a permanent feed of fresh reactants. Using an autocatalytic bistable but nonoscillatory reaction, namely, the bromate-sulfite reaction, we predict that a piece of hydrogel that swells/shrinks as a function of  $pH$  can exhibit spontaneous mechanical and chemical oscillations. This constitutes the extension to realistic and experimentally feasible conditions of results previously obtained on a toy model with artificial swelling conditions.

**PACS.** 82.40.Ck Pattern formation in reactions with diffusion, flow and heat transfer – 82.40.Bj Oscillations, chaos, and bifurcations – 82.33.Ln Reactions in sol gels, aerogels, porous media

## 1 Introduction

The swelling of gels under the action of external physical or chemical parameters is raising a growing interest in view of multiple potential applications in sensors, actuators, biomimetic systems or drug delivery. Among swelling agents able to induce swelling, the chemical composition of the solvent has received particular attention [1–5]. In this article, we consider the coupling of chemical reactions with chemo-responsive gels as a source of spontaneous mechanical oscillations. Different strategies to get such mechanical oscillations have been used. In all cases, a small piece of hydrogel that swells/shrinks as a function of the composition of the solvent is plunged in a solution of chemicals in large excess or permanently fed with fresh reactants. These reactants diffuse into the gel where the reaction is going on and drive the swelling process. More extensive reviews than the following short introduction will be found in [5]. First, one can immerse a piece of gel in an oscillating reaction carried out in a continuous stirred tank reactor (CSTR) or a large reservoir. The periodic changes of concentrations induce periodic swelling/shrinking cycles of the gel [6,7]. The process was simulated with toy models by Villain *et al.* [8,9]. Alternatively, one can attach to the gel a catalyst necessary for the reaction to oscillate by grafting it on the polymer network. This has been done for the Belousov-Zhabotinskii reaction (BZ) by Yoshida and coworkers [10–12] and a model has been proposed by Yashin and Balasz [13]. In this case, only the gel

and its contents are oscillating since the required conditions are only fulfilled within it. However, in both cases, the source of the oscillations is a purely chemical instability. Mechanical oscillations are slaved to chemical oscillations that would also occur in an inert gel (apart from slight changes due to the dilution of the catalyst during swelling). Unfortunately, oscillating reactions remain rare and the domain of parameters where oscillations occur is often very small.

Other strategies based on bistability and on the associated hysteresis, a common phenomenon in nonlinear physics, have been proposed. The basic principle is to create a feedback that makes both states slightly unstable so that the system permanently switches between them, following periodically the hysteresis cycle. Siegel *et al.* use the hysteresis of the volumic transition in a membrane made of a gel responsive to  $pH$  to modulate its porosity and the coupling through this membrane of two compartments where an autocatalytic reaction takes place, leading to chemical oscillations [14–16]. Instead, we proposed to take advantage of chemical bistability and to use the volume changes caused by swelling/shrinking as a feedback [17–19]. This was partly supported by a series of experiments performed with the chlorite-tetrathionate (CT) reaction in a poly(NiPAA-co-AA) gel [20–22]. We shall now focus on this approach.

Although our former works [17–22] have clearly demonstrated the validity of chemical spatial bistability as a potential source of oscillations, there were still two sorts of problems to be solved to get a coherent whole. First, even in a nonresponsive gel, the CT reaction exhibits,

<sup>a</sup> e-mail: boisson@crrp-bordeaux.cnrs.fr

in addition to spatial bistability, complex dynamics [23] which perturbs the interpretations. Moreover, although a description in terms of effective diffusion coefficients is sufficient to understand the essential dynamics, the kinetic model breaks down when the motion of ionic charges is accounted for. The choice of a more appropriate reaction is advisable. The second problem is also fundamental. In our former toy models, the gel swelling properties were related to the chemical composition of the solvent in a heuristic way through an arbitrary dependence of the Flory parameter  $\chi$  with one of the concentrations. More satisfactory models should rely on a more pertinent description of the swelling source. In pH-sensitive polyelectrolytes, the most commonly used responsive hydrogels, the swelling is induced by the osmotic pressure due to the partial ionisation of the polymer network. The purpose of this article is to demonstrate that occurrence of oscillations that originate in pure chemo-mechanical instabilities based on spatial chemical bistability can be predicted on the basis of reasonable and more realistic models. We shall use the Bromate-Sulfite reaction (BS) for which a good kinetic model is available [24, 25] and we shall develop a model of swelling for a polyelectrolyte in the presence of the reaction. Beforehand, we shall briefly summarize the principles of the chemo-mechanical instability. For more extensive developments on spatial bistability, see [23, 26] and on the chemo-mechanical instability itself, see [18, 19, 23].

Many autocatalytic reactions carried out in a CSTR exhibit bistability as a function of the residence time  $t_{\text{res}}$  [27]. At short  $t_{\text{res}}$ , the extent of reaction  $\xi$  is low. The reaction time is longer than the time to refill the reactor with fresh reactants and the composition remains close to the concentrations in the input flow. On the opposite, for a long  $t_{\text{res}}$ ,  $\xi$  is large and the reaction is almost completed. At intermediate values of  $t_{\text{res}}$ , there are two stable states, one with low  $\xi$  (the “flow” state F) and the other with large  $\xi$  (the “thermodynamic” state T) selected according with the previous history of the system. If a piece of a chemically inert gel, plunged in the same almost unreacted medium —most often a CSTR kept in the F state— a similar phenomenon called “spatial bistability” occurs as a function of the typical size  $l$  of the gel. This parameter, which determines the time to transport by diffusion the reactants to the deep core of the gel, plays a role analog to  $t_{\text{res}}$ . If  $l$  is small, exchanges with the environment are faster than reaction rates. The whole gel remains in a state close to the reservoir (low  $\xi$ ) and is again referred to as a flow state (F). If  $l$  is large, the reaction becomes dominant at some distance of the boundary, so that the deep core of the gel is at large  $\xi$ , except for a boundary layer that ensures continuity of concentrations with the reservoir. This defines the “mixed state” M. At intermediate sizes  $l_{\text{inf}} < l < l_{\text{sup}}$ , both states can be stable, which defines the spatial bistability. A number of reactions have already been shown to exhibit this phenomenon [23, 25, 28–30]. Obviously, other parameters such as a concentration in the feeding medium can be used to define the bistability domain, but  $l$  is the most relevant to our goal. If one could slowly and continuously increase  $l$ , starting from  $l < l_{\text{inf}}$ , one could follow the F

state branch until the system switches to the M state at  $l = l_{\text{sup}}$ . If, now, we reverse this change,  $l$  decreases and the system follows the M branch down to  $l = l_{\text{inf}}$ , where it switches back to the F state. In this way, one follows the whole hysteresis cycle associated to the spatial bistability. If we replace the inert gel by a chemo-responsive gel, the changes of size  $l$  are spontaneously driven by the chemical state. For instance, in the BS reaction that will be studied further, the F state is alkaline and tends to make the polyacid gel swell, whereas the M state is mainly acid and tends to make the gel shrink. If  $l$  is appropriate and the swelling/shrinking process is slow enough in regard to the reaction-diffusion process, one can start on state F, swell up to  $l = l_{\text{sup}}$ , switch to state M, shrink down to  $l = l_{\text{inf}}$ , and switch back to state F. The process is repeated indefinitely, leading to periodic oscillations both of the volume of the gel and of the concentrations within the gel. One does not need an oscillating reaction, only a much more common bistable one, to produce such a chemo-mechanical instability. Some models have been proposed to predict the dynamics of swelling in neutral gels without reaction [31–37] or with reaction [9, 13, 18, 19]. In the second case, the chemical sensitivity of the gel is described by an assumed and somewhat arbitrary dependence of the Flory parameter  $\chi$ , which gathers all the energetic interactions of monomer and solvent molecules, on the concentration of a chemical species. However, most gels that exhibit large volume variations are polyelectrolytes that mainly swell under the action of the ionic osmotic pressure [38–40]. Only a few dynamical complex models have been developed to simulate the swelling of polyelectrolytes in the presence of simple ionic reactions [41, 42]. With complicated reactions implying both ions and neutral species, the situation is still more complex in regard to the number of involved primary and secondary phenomena with unknown parameters. Thus, to work out a model that could be applied to a realistic reaction, namely, the BS reaction, we had to resort to some simplifications.

In this article, we consider a piece of gel immersed in a CSTR kept in the F state by a permanent feed of fresh reactants. The equations are general but will be eventually applied to the BS reaction. We limit ourselves to a one-dimensional (1-D) system. A gel swelling in a capillary is not very realistic from an experimental point of view but a good approximation to such a 1-D system could be obtained by grafting a flat piece of gel on the bottom of the reactor, provided that the thickness  $l$  is much smaller than the size in the transverse directions for the effects of the deformations in these directions to be limited to the edges and to be neglected. In Section 2, we introduce a simple model for the mechanism of swelling of the polyelectrolyte in the presence of a reaction. In Section 3, we establish generalized reaction-diffusion equations within such a gel. In Section 4, some aspects of the spatial bistability of the BS reaction are discussed. In Section 5, we gather all the elements of the model and perform the numerical simulation which demonstrates that chemo-mechanical oscillations of the type described above can actually be predicted. In an inert gel, the model previously developed for the kinetics and transport in the BS reaction is in good

agreement with experimental data [25]. Its extension to the swelling gel remains more likely valid, but modeling the swelling process itself needs a simplified description in which only the main contributions are accounted for. Thus, it must be clear that we do not claim that we give an almost exact quantitative modeling of the dynamics, but we believe that this approach captures the main phenomena, the orders of magnitude, and the general trends. It should be considered as a first guide for experimentalists.

## 2 The swelling model

There are three types of constituents in the gel: the solvent (water), the polymer, and the solutes (the chemicals).

The concentrations  $c_i$  of the chemicals are low so their volume fraction is assumed to be negligible in regard to the volume fraction  $\phi$  of the polymer and the volume fraction  $1 - \phi$  of the solvent. The polymer is assumed to be a polyacid. The concentration of ionisable sites in the polymer in the absence of solvent would be  $c_{a0}$ , so that their concentration in the gel is given by  $c_a = \phi c_{a0}$ . In the referential of the laboratory, the dynamics at a given point in the gel are characterized by the velocity of the polymer matrix  $\mathbf{v}_P$ . The permeation flow of the solvent through the polymer matrix is associated to the relative velocity  $\delta\mathbf{v} = \mathbf{v}_P - \mathbf{v}_S$ , where  $\mathbf{v}_S$  is the velocity of the solvent in the same referential. In common hydrogels, the total network+solvent system satisfies the incompressibility condition. Then, in systems with stagnation points or fixed walls (like here), the equation for mass balance expressed in terms of volume fractions is given by the conservation law

$$\phi\mathbf{v}_P + (1 - \phi)\mathbf{v}_S = 0, \quad (1)$$

which allows to express  $\mathbf{v}_S$  and  $\delta\mathbf{v}$  as a function of  $\mathbf{v}_P$ . The local force density acting on the polymer matrix is given by  $\mathbf{f} = \nabla \cdot \bar{\sigma}$ , where  $\bar{\sigma}$  is the stress tensor. These forces result from the form of the free energy associated to the mixing of the polymer molecules with the solvent molecules, from the elastic forces exerted by the network when deformations are applied, and from those associated to the partial ionisation of the network. The stress tensor can be splitted in two parts that correspond, respectively, to an isotropic contribution and an anisotropic contribution in the form

$$\sigma_{ij} = \underbrace{-\delta_{ij}\Pi}_{\text{isotropic}} + \underbrace{\sigma_{ij}^{(\text{noniso})}}_{\text{nonisotropic}}, \quad (2)$$

where  $\Pi$  can be considered as a pressure and is commonly referred to as the ‘‘osmotic pressure’’. It can be decomposed in three terms corresponding to the three sources of forces:

$$\Pi = \Pi_{\text{mix}} + \Pi_{\text{elas}} + \Pi_{\text{ion}}. \quad (3)$$

For a unidimensional deformation, there is only one coordinate and the anisotropic part of the stress tensor, which is only due to the elastic forces, can be included in the elastic contribution  $\Pi_{\text{elas}}$  to the osmotic pressure. Then,

the system is at equilibrium when  $\Pi = 0$ . Out of equilibrium, the osmotic forces are counterbalanced by the friction forces exerted by the solvent on the network and proportional to their relative velocity  $\delta\mathbf{v}$

$$\begin{aligned} \text{Friction forces} &= \text{Osmotic forces} \\ \zeta(\phi)\delta\mathbf{v} &= -\nabla\Pi, \end{aligned} \quad (4)$$

where  $\zeta(\phi)$  is a friction coefficient which increases with  $\phi$ . The exact shape of this function is not well known. Many authors use a dependence in  $\phi^{3/2}$  on the basis of theoretical arguments only valid for semidilute polymers. At the low polymer densities on which we focus, we have preferred the Ogston model based on flow analysis in fiber networks [43], as proposed in [34]

$$\zeta(\phi) = \frac{RT}{V_S} \frac{1}{D_0} \phi e^{\eta\sqrt{\phi}}, \quad (5)$$

where  $\eta$  is of the order of the ratio of the radius of the polymer chains to the size of the solvent molecule and  $V_S$  the molar volume of the solvent. In the original theory,  $D_0$  should be the autodiffusion coefficient of this solvent but it was found in swelling experiments that the actual value should be almost two orders of magnitude larger [34]. Thus, we shall consider  $D_0$  as an expandable parameter in the range  $0.01 \text{ mm}^2/\text{s} \leq D_0 \leq 0.1 \text{ mm}^2/\text{s}$ .

The mixing term is written in agreement with the classical Flory-Huggins theory [38, 44]

$$\Pi_{\text{mix}} = -\frac{RT}{V_S} [\phi + \log(1 - \phi) + \chi\phi^2]. \quad (6)$$

The first two terms depend on the entropy of mixing, the third one depends on the mutual energetic interactions between the different molecules (solvent and monomers). A more rigorous theory would need to introduce virial coefficients specific to each gel [45]. Large swelling generally occurs when  $\chi$  is slightly larger than 0.5. There has been a great number of debates about the form of the elastic terms without definite and universal answer. At our level of description and in the absence of precise experimental data —to be determined for each composition of gel— we shall follow the simple phenomenologic approach of Barrière and Leibler [35] based on the work of Bastide and Candau [46]. The authors assert that both the free energy by unit volume and the elastic modulus  $G(\phi)$  scale like  $(\phi/\psi)^n$ . To fit at best with other theories and recover Flory’s expressions [38], we use  $n = 1/3$  and  $\psi = \phi_0$  where the reference state of volume fraction  $\phi_0$  is supposed to be in a relaxed state (normally a condensed state before swelling). During swelling, the network experiences deformations and a point  $i$  of initial coordinate  $X_i$  is moved to coordinate  $x_i$  at time  $t$ . In the following, we consider the relaxed state as an initial undeformed state. To remain unidimensional during swelling, the gel has to be constrained by external walls or grafting. This implies that, contrary to a gel that swells freely in its solvent, the final equilibrium is not an isotropic state. The local deformation at point  $i$  and time  $t$  is measured in a

1-D system by  $dx_i/dX_i$ . The unidirectional transformation  $dX_i \rightarrow dx_i$  can be decomposed in a virtual isotropic swelling  $dX_i \rightarrow dx'_i$  followed by an anisotropic stretching  $dx'_i \rightarrow dx_i$  imposed by the constraints at constant volume with deformation  $\lambda = dx'_i/dx_i$ . Thus

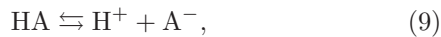
$$\frac{\phi_0}{\phi} = \frac{dx_i}{dX_i} = \frac{dx_i}{dx'_i} \frac{dx'_i}{dX_i} = \lambda \left( \frac{\phi_0}{\phi} \right)^{\frac{1}{3}} \Rightarrow \lambda = \left( \frac{\phi_0}{\phi} \right)^{\frac{2}{3}}. \quad (7)$$

On the basis of the above assertions, the following expression can be derived [35]:

$$\Pi_{\text{elas}} = -K_{\text{net}} \frac{RT}{V_S} \left( \frac{\phi}{\phi_0} \right)^{\frac{1}{3}} \left[ 1 + C_\lambda \left( \lambda^2 - \frac{1}{\lambda} \right) \right], \quad (8)$$

where  $K_{\text{net}}$  is a constant which depends on the network properties and  $C_\lambda$  is a constant of order unity proportional to the shear modulus  $G(\phi)$ . The terms that contain  $\lambda = (\phi_0/\phi)^{\frac{2}{3}}$  represent the nonisotropic contribution to the osmotic pressure.

To give an expression for  $\Pi_{\text{ion}}$ , we shall first consider the equilibrium. In accordance with many authors [40], we neglect, in this simple approach, all the electrostatic interactions between the ions in the network to keep only the entropy terms that should be dominant. We closely follow the approach of Rička and Tanaka [39]. In the gel, the ionisable monomers HA, the concentration of which is  $c_{a0}\phi$  in the absence of dissociation, are actually partly ionised into  $\text{H}^+$  and  $\text{A}^-$  according to



with the equilibrium constant

$$K_g = \frac{[\text{H}^+][\text{A}^-]}{[\text{HA}]}. \quad (10)$$

From equation (10), one gets

$$c_a = \frac{K_g c_{a0} \phi}{K_g + [\text{H}^+]}. \quad (11)$$

Whereas other ions are mobile, the ions  $\text{A}^-$  are attached to the network. According to the classical theory of the Donnan equilibrium, this creates an excess of mobile ions in the gel in regard to their concentrations in the surrounding medium (here, the CSTR contents). This creates in turn a pressure difference, which, for small concentrations is analog to the pressure created by a perfect gas

$$\Pi_{\text{ion}} = RT \sum_i (c_i - c'_i), \quad (12)$$

where the sum was taken on the mobile ions, the  $c'_i$ 's are the concentration of these ions in the CSTR and the affinities have been replaced with the concentrations. To cross the boundary, the ions have to go through a potential difference  $\delta U$  in agreement with the Boltzman law

$$\frac{c_i}{c'_i} = \exp \left( -\frac{z_i e \delta U}{k_B T} \right) = K^{z_i}, \quad (13)$$

where  $e$  is the charge of the electron,  $z_i$  is the charge number of ion  $i$  and  $K$  is the Donnan ratio, which is common to all mobile ions. Given the  $c'_i$ 's, and using equations (6, 8, 11–13), one can compute  $K$  and  $\phi$  by solving numerically the system of two nonlinear equations which respectively express electroneutrality in the gel and mechanical equilibrium:

$$\sum_i c_i z_i + z_a c_a = 0 \quad (\text{electroneutrality}), \quad (14)$$

$$\Pi = 0 \quad (\text{mechanical equilibrium}), \quad (15)$$

where the charge number of  $\text{A}^-$  is  $z_a = -1$ . The concentrations of nonionic species are continuous at the boundary. To solve the dynamical equations, we assume that the system is at local Donnan equilibrium at the CSTR boundary so that, at this point,  $\Pi_{\text{ion}}$ ,  $\phi$  and  $K$  can be computed as explained above. Consequently, all the  $c_a$  and  $c_i$ 's concentrations are obtained from equations (11) and (13). This defines completely the boundary condition. Inside the gel, the generalisation of the calculation of  $\Pi_{\text{ion}}$  is not straightforward, because the reaction creates or destroys not only ions but also neutral molecules. One can assume that the ionic osmotic pressure is proportional to the degree of ionisation of the polymer which can be written in the form

$$\Pi_{\text{ion}} = K_{\text{ion}} c_a. \quad (16)$$

To remain consistent, at the CSTR boundary,  $\Pi_{\text{ion}}$  computed from equation (16) must be equal to the value already computed from equation (12). Thus, the value of  $K_{\text{ion}}$  is obtained from equation (16) where  $c_a$  and  $\Pi_{\text{ion}}$  at the boundary are, respectively, obtained from equations (11) and (12).

If the distribution of concentrations and  $\phi$  at time  $t$  is known, it is now possible to compute  $\Pi$  at each point inside the gel. Then, from equations (1) and (4), one gets the velocity of the polymer

$$\mathbf{v}_P = -\frac{(1-\phi)}{\zeta(\phi)} \nabla \Pi \quad (17)$$

and the velocity of the solvent

$$\mathbf{v}_S = -\frac{\phi}{(1-\phi)} \mathbf{v}_P. \quad (18)$$

Taking into account the equation of conservation for the polymer

$$\frac{\partial \phi}{\partial t} + \nabla \cdot (\mathbf{v}_P \phi) = 0, \quad (19)$$

one gets the dynamical equation for  $\phi$

$$\frac{\partial \phi}{\partial t} = \nabla \cdot \left( \frac{\phi(1-\phi)}{\zeta(\phi)} \nabla \Pi \right). \quad (20)$$

As equation (17), equation (20) describes the motion of the polymer matrix through the evolution of the gel density. To solve our problem, one needs now to couple equation (20) to the equations that describe the reaction and the transport of the chemical species in the gel.

### 3 The transport model

Inside the gel, the species are transported by three processes, namely, migration due to the internal electric field, diffusion, and convective motions due to swelling. Our main hypothesis is that the solutes, indexed by  $i$  or  $k$ , are convected like the solvent (*i.e.* at velocity  $\mathbf{v}_S$ ), whereas the anion  $A^-$ , indexed by  $a$ , is attached to the network and is obviously convected like the polymer (*i.e.* at velocity  $\mathbf{v}_P$ ). The transport model is a straightforward generalisation of the transport equations for electrolytes as presented by Newman [47]. The fluxes are given by the equations

$$\mathbf{N}_i = \overbrace{-Fz_i u_i \nabla U}^{\mathbf{N}_{mi}} - D_i \nabla c_i + c_i \mathbf{v}_S, \quad (21)$$

$$\mathbf{N}_a = c_a \mathbf{v}_P, \quad (22)$$

where  $F$  is the Faraday constant,  $u_i$  is the mobility of species  $i$ ,  $D_i$  its diffusion coefficient, and  $U$  is now the diffusion potential created by the distribution of charges when the diffusion coefficients of the ions are not all equal [47]. In the expression of  $\mathbf{N}_i$ , the first term  $\mathbf{N}_{mi}$  corresponds to migration, the second term to diffusion, and the late term to convection. The current density is

$$\mathbf{j} = F \left( \sum_i z_i \mathbf{N}_i + z_a \mathbf{N}_a \right). \quad (23)$$

Taking into account equations (21) and (22) and the electroneutrality condition

$$\sum_i z_i c_i + z_a c_a = 0, \quad (24)$$

one gets

$$\mathbf{j} = -\kappa \nabla U - F \sum_i z_i D_i \nabla c_i + F \delta \mathbf{v} z_a c_a, \quad (25)$$

where the conductivity  $\kappa$  is defined by  $\kappa = F^2 \sum_i z_i^2 u_i c_i$ . There is no permanent current, so that, writing  $\mathbf{j} = 0$  in equation (25), one can eliminate the potential  $U$  from equation (21). We define the transference numbers

$$t_i = \frac{z_i^2 D_i c_i}{\sum_i z_i^2 D_i c_i}, \quad (26)$$

where the diffusion coefficients replace the mobilities since, according to the Nernst-Einstein relation, one has  $D_i = RT u_i$ . The migration flux  $\mathbf{N}_{mi}$  becomes:

$$\mathbf{N}_{mi} = \frac{t_i}{z_i} \left( \sum_k z_k D_k \nabla c_k - z_a c_a \delta \mathbf{v} \right). \quad (27)$$

One can also eliminate one ion, indexed by  $n$ , from this expression by rewriting the electroneutrality condition under the form

$$-z_n c_n = \sum_{k \neq n} z_k c_k + z_a c_a. \quad (28)$$

It is advisable to use a nonreactive ion with a well-known diffusion coefficient  $D_n$ . This is generally  $\text{Na}^+$  or  $\text{K}^+$  which are often the cation of input reactive salts but which, most of the time, remain spectators of the reaction, being only involved in the transport by their electric charge. The final expression for  $\mathbf{N}_{mi}$  is

$$\mathbf{N}_{mi} = \frac{t_i}{z_i} \left( \sum_{k \neq n} z_k (D_k - D_n) \nabla c_k - D_n z_a \nabla c_a - z_a c_a \delta \mathbf{v} \right). \quad (29)$$

The diffusion coefficients of the solutes depend on the volume fraction  $\phi$  of the polymer. The diffusion coefficient is proportional to the ratio  $\epsilon/\tau$  of the permittivity to the tortuosity. Since we shall only consider small polymer densities  $\phi \ll 1$ , we assume that both  $\epsilon$  and  $\tau$  depend linearly on  $\phi$ . The available volume fraction for the solutes is  $1 - \phi$ , so that we can write  $\epsilon = 1 - \phi$ . For the tortuosity, one has  $\tau = 1 + \alpha\phi$ , where  $\alpha$  is a coefficient of order unity (3/2 for a periodic network of spheres [48]). For diffusion, the network can be seen as a random network of fibers. Extrapolating the numerical simulations of Tomadakis and Sotirchos [49] to  $\phi \rightarrow 0$ , one finds  $\alpha \approx 1$ . Thus, if  $D_{0i}$  is the diffusion coefficient of species  $i$  in pure solvent, we get

$$D_i(\phi) \approx D_{0i} \frac{1 - \phi}{1 + \phi} \approx D_{0i} (1 - 2\phi). \quad (30)$$

In the computations, we shall use  $D_i(\phi) = D_{0i} (1 - 2\phi)$ .

The evolution of the concentrations is given by the conservation laws

$$\frac{\partial c_i}{\partial t} = -\nabla \cdot \mathbf{N}_i + R_i, \quad (31)$$

$$\frac{\partial c_a}{\partial t} = -\nabla \cdot \mathbf{N}_a + R_a, \quad (32)$$

where  $R_i$  and  $R_a$  are the reaction terms ruled by the chemical kinetics and  $N_i$  and  $N_a$  are obtained from equations (21, 22), and (29).

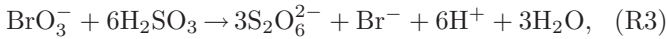
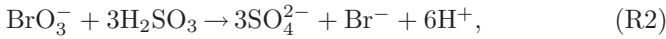
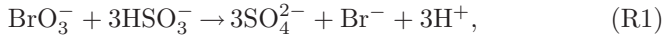
These transport equations are general. In the next section, we introduce the kinetic terms  $R_i$  and  $R_a$  for the BS reaction.

## 4 The reaction model

### 4.1 Kinetic equations for the BS reaction

The bromate-sulfite model is a reaction which is autocatalytic with  $\text{H}^+$  and has been studied previously both in CSTR [24] and in the context of spatial bistability [25]. The reader is invited to refer to [25] for details on the kinetic model and the experimental procedures. We shall here report the essentials to understand the next section. The gel is in contact with the contents of a CSTR fed with solutions of bromate, sulfite and sulfuric acid at a residence time  $\tau = 500$  s. The volume of the CSTR is assumed to be large enough in order that the reaction inside is not significantly influenced by the gel contents.

The kinetics equations, kinetic constants, and diffusion coefficients are the same as those used in [25] except for an additional reaction to account for the dissociation of the gel according to equation (9). The  $pK$  of the polyacid has been fixed to 5.5 which should correspond to the  $pK$  of a gel of poly(N-isopropylacrylamide-co-acrylic acid) (NiPAAM-co-AA) which is commonly used in swelling and chemo-mechanics experiments. The kinetics are described by a series of balance equations completed by fast equilibria



with the corresponding rate laws

$$\begin{aligned} r_1 &= k_1[\text{HSO}_3^-][\text{BrO}_3^-], \\ r_2 &= k_2[\text{H}_2\text{SO}_3][\text{BrO}_3^-], \\ r_3 &= k_3[\text{H}_2\text{SO}_3][\text{BrO}_3^-], \\ r_4 &= k_4[\text{SO}_3^{2-}][\text{H}^+] - k_{-4}[\text{HSO}_3^-], \\ r_5 &= k_5[\text{HSO}_3^-][\text{H}^+] - k_{-5}[\text{H}_2\text{SO}_3], \\ r_6 &= k_6[\text{SO}_4^{2-}][\text{H}^+] - k_{-6}[\text{HSO}_4^-], \\ r_7 &= k_7[\text{HSO}_4^-][\text{H}^+] - k_{-7}[\text{H}_2\text{SO}_4], \\ r_8 &= k_8[\text{H}^+][\text{OH}^-] - K_w, \\ r_9 &= k_9[\text{H}^+][\text{A}^-] - k_{-9}[\text{HA}]. \end{aligned} \quad (33)$$

The constants and the diffusion coefficients in pure water used in the numerical simulations are, respectively, given in Table 1 and Table 2. When they were unavailable in the literature, the diffusion coefficients were fixed to reasonable values and are marked with an asterisk. Results on spatial bistability in a nonresponsive and chemically inert gel have been reported in [25]. The introduction of reaction (R9) could modify the results. In order to well distinguish effects of the sole chemistry from those of chemo-mechanical instabilities, and also check that the parameters requirements for the emergence of such instabilities are still fulfilled, we have repeated some of the previous simulations when a nondiffusive complexing agent such as  $\text{A}^-$  is present inside the nonresponsive gel, but not in the CSTR. In these preliminary computations, the purpose is to check the sole possible influence of the presence of the complex HA. Thus, as in [25], the volume fraction of the gel is neglected. The concentration  $[\text{HA}]_0$  before dissociation was fixed to  $5 \times 10^{-2}$  M, that will be the typical mean value for  $c_{a0}\phi$  that will be obtained for the mechanically responsive polyelectrolytes in the next section.

**Table 1.** Kinetic constants used in the numerical simulations.

$k_1 = 0.0653 \text{ M}^{-1} \text{ s}^{-1}$	
$k_2 = 18 \text{ M}^{-1} \text{ s}^{-1}$	
$k_3 = 0.7 \text{ M}^{-1} \text{ s}^{-1}$	
$k_4 = 5 \times 10^{10} \text{ M}^{-1} \text{ s}^{-1};$	$k_{-4} = 3 \times 10^3 \text{ s}^{-1}$
$k_5 = 2 \times 10^8 \text{ M}^{-1} \text{ s}^{-1};$	$k_{-5} = 3.4 \times 10^6 \text{ s}^{-1}$
$k_6 = 1. \times 10^{10} \text{ M}^{-1} \text{ s}^{-1};$	$k_{-6} = 1. \times 10^3 \text{ s}^{-1}$
$k_7 = 1 \times 10^{11} \text{ s}^{-1};$	$k_{-7} = 1.148 \times 10^9 \text{ M}^{-1} \text{ s}^{-1}$
$k_8 = 1.4 \times 10^{11} \text{ M}^{-1} \text{ s}^{-1};$	$K_w = 10^{-14} \times k_8$
$k_9 = 1 \times 10^{10} \text{ M}^{-1} \text{ s}^{-1};$	$k_{-9} = 10^{-5.5} \times k_8 \text{ M}^{-1} \text{ s}^{-1}$

**Table 2.** Diffusion coefficients. Asterisks correspond to values used for unavailable coefficients.

Species	$z_i$	$D_i \times 10^5 \text{ cm}^2 \text{ s}^{-1}$
$\text{H}^+$	+1	9.312
$\text{BrO}_3^-$	-1	1.485
$\text{SO}_3^{2-}$	-2	1.1*
$\text{HSO}_3^-$	-1	1.5*
$\text{OH}^-$	-1	5.26
$\text{SO}_4^{2-}$	-2	1.065
$\text{HSO}_4^-$	-1	1.33
$\text{S}_2\text{O}_6^{2-}$	-2	1.0*
$\text{Br}^-$	-1	2.084
$\text{H}_2\text{SO}_3$	0	1.6*
$\text{Na}^+$	+1	1.334

## 4.2 Spatial bistability of the BS reaction in the presence of a complexing agent

The concentrations in the input flow, indexed by 0, are always chosen in order that the CSTR remains in the flow state, *i.e.* slightly basic. The F and M states in the gel are characterized by the  $pH$  at the bottom of the gel: basic or quasi-neutral for state F, acid ( $pH \sim 3$ ) for state M. The concentrations at the CSTR/gel boundary ( $x = l$ ) are derived in agreement with the rules of Donnan equilibrium. The concentrations in the CSTR being first computed, the Donnan ratio  $K$  is computed according to the procedure described in Section 2 to determine the fixed concentration within the gel at the CSTR boundary. Since  $\phi = 0$ , only equation (14) has to be solved with  $c_a = K_g[\text{HA}]_0 / (K_g + [\text{H}^+])$  and the  $c_i$ 's are given by equation (13). No flux boundary conditions are applied at the opposite wall ( $x = 0$ ). We found that the presence of the complexing agent does not preclude spatial bistability. In Figure 1 a typical bistability diagram in the plane ( $[\text{H}_2\text{SO}_4]_0, l$ ) is shown, where  $l$  is the size of the 1-D system. For a given set of input concentrations, the range of sizes  $l$  for which the system is bistable is an essential parameter for the emergence of chemo-mechanical oscillations. We found that these limits of the bistability region are almost independent of  $[\text{HA}]_0$  in the range of concentrations we shall consider in the following section.

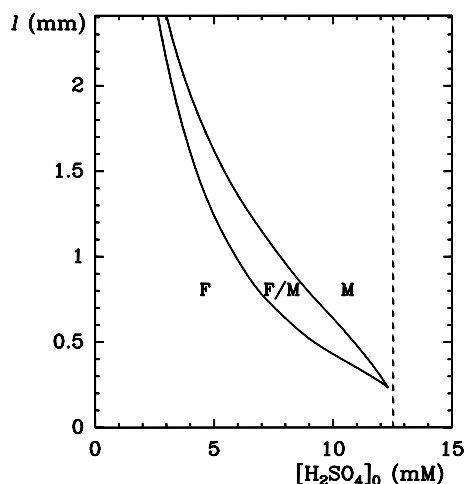


**Fig. 1.** Nonequilibrium state diagram. F: flow state. M: mixed state. F/M: spatial bistability. CSTR input flows:  $[\text{BrO}_3^-]_0 = 25$  mM,  $[\text{SO}_3^{2-}]_0 = 60$  mM.

For information, we also report in Figure 2 the concentration profiles of  $\text{H}^+$  and  $c_a$  in states F and M for a set of data within the bistability range. The system was previously found to exhibit marginal oscillations in a very narrow domain of parameters for large values of  $[\text{BrO}_3^-]_0$ . However, it is known that, for most oscillatory reactions, complexation of the catalyst generally kills oscillations whereas bistability is preserved. This is actually the case. We have checked that these marginal oscillations are totally killed in the polyelectrolyte gel and that the oscillations that will be evidenced in the next section are of pure chemo-mechanical origin.

## 5 Chemo-mechanical oscillations

We now couple the chemical reactions with gel swelling, solving simultaneously equations (20, 31, 32), where the  $R_i$ 's and  $R_a$  are given by equations (33) and the expressions of  $\nabla\Pi$ ,  $N_i$ , and  $N_a$  are computed as explained in the previous sections.

### 5.1 Numerical techniques

To solve these equations, it is appropriate to switch to a Lagrangian representation on a fixed grid with a uniform volume fraction  $\phi_0$ , size  $l_0$ , and a constant spatial stepsize  $\delta X_i$ . In this 1-D system, the transformation from Eulerian coordinates  $x$  to Lagrangian coordinates  $X$  is operated by the simple transformation

$$x \longrightarrow X \quad \Longrightarrow \quad \nabla_x \longrightarrow \frac{\phi}{\phi_0} \nabla_X \quad (34)$$

in the equations. At each time, one can recover the value of  $x_i$  corresponding to the point of coordinate  $X_i$  in the fixed grid from the equation

$$x_i = \int_0^{X_i} \frac{\phi_0}{\phi(X)} dX \quad (35)$$

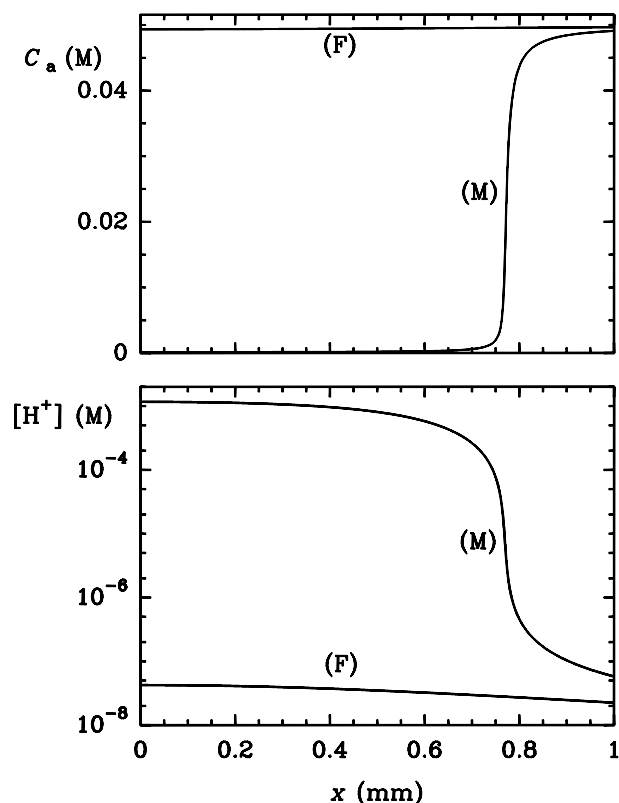


**Fig. 2.** Concentration profiles of  $\text{H}^+$  and  $c_a$  in the gel. F: flow state. M: mixed state. F/M: spatial bistability. CSTR input flows:  $[\text{BrO}_3^-]_0 = 25$  mM,  $[\text{SO}_3^{2-}]_0 = 60$  mM,  $[\text{H}_2\text{SO}_4^{2-}]_0 = 6.5$  mM,  $l = 1$  mm.

to get the values of  $c_i(x_i)$  and  $\phi(x_i)$  in Eulerian coordinates from  $c_i(X_i)$  and  $\phi(X_i)$ . The integration on the Lagrangian fixed grid is performed with finite differences and a method of lines based on a stiff fourth-order Rosenbrock temporal integrator [50].

### 5.2 Parameters choice

We limit ourselves in this presentation to the complete determination of the oscillatory domain in a  $([\text{H}_2\text{SO}_4]_0, l_0)$  plane of the phase diagram for a unique representative set of the other parameters.

Chemical parameters are archetypal of those that were used in spatial bistability studies of the BS reaction. As for computational results reported in Figure 1, the bromate and sulfite concentrations in the input flow are respectively fixed to  $[\text{BrO}_3^-]_0 = 25$  mM and  $[\text{SO}_3^{2-}]_0 = 60$  mM. Only the reference size  $l_0$  of the relaxed gel and  $[\text{H}_2\text{SO}_4^{2-}]_0$  are systematically varied.

The choice of gel parameters is more problematic and is only guided by the necessity to ensure that both the values of these parameters and the swelling amount are similar to those encountered in typical experiments. The reference volume fraction  $\phi_0$  is assumed to be the value of  $\phi$  in a fully contracted gel (acid medium). Since the gel must be diluted (typically a few percent in the experiments), we take  $\phi_0 = 0.05$ . To account for the shearing

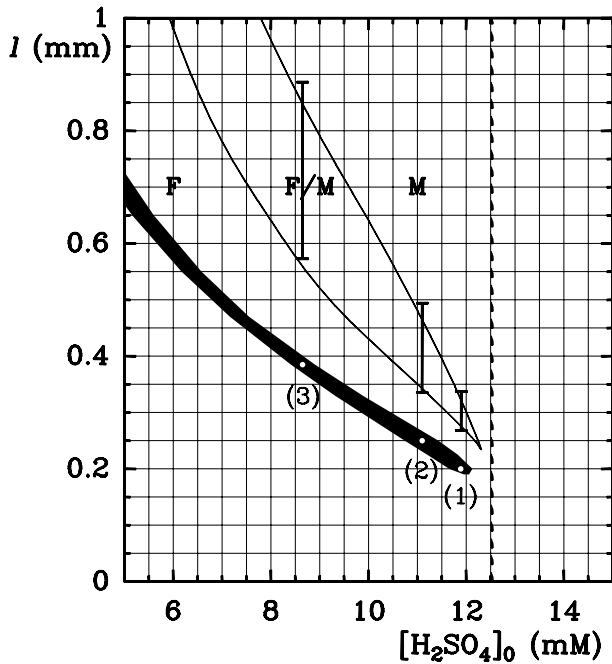


**Fig. 3.** Nonequilibrium state diagram of oscillatory chemo-responsive gel. Black zone: oscillatory behavior ( $l$  is  $l_0$ ). Vertical bars are covering the variations of gel size  $l$  during an oscillation for three parameters sets (white points). The indicative limits of spatial bistability for fixed size are reported from Figure 1.

effects, we use equation (8) with  $C_\lambda=1$  as in [35]. To produce a significant swelling amount without a full volume transition, the Flory parameter is fixed to  $\chi = 0.515$ , *i.e.* a value slightly larger than  $1/2$ , and the corresponding value of  $K_{\text{net}}$  is obtained in the relaxed state (no stress) from

$$K_{\text{net}} = -[\phi_0 + \log(1 - \phi_0) + \chi\phi_0^2]\phi_0^{-\frac{1}{3}}. \quad (36)$$

As in Section 4, the  $pK_a$  of the gel is fixed to 5.5, the value generally retained for the poly-N-isopropylacrylamide-co-acrylic acid (NiPAAM-co-AA) gels. In the simulations reported in the next paragraph, the coefficients of equation (5) are fixed to  $D_0 = 0.03 \text{ mm}^2/\text{s}$  and  $\eta = 5$ . In these computations, the size of the gel is changing during time. As a size reference for a given system, we use  $l_0$ , the size in the fully contracted state, *i.e.* at volume fraction  $\phi_0$ . Since there is always a part of the gel which is in a swollen state, at least in the region close to the CSTR/gel boundary, the real size  $l(t)$  at a given instant  $t$  is always larger than this value.

### 5.3 Simulation results

The domain where oscillations are actually observed is mapped out as a black region in the  $([H_2SO_4]_0, l_0)$  parameter plane (Fig. 3). In the definition of this region, the ordinate  $l$  must be understood as the reference length  $l_0$ . The actual range of sizes covered during the oscillations for three representative sets of parameters (white

**Table 3.** Amplitude and period of oscillations.

Point	$[H_2SO_4]_0$ (mM)	$l_0$ (mm)	$l_m$ (mm)	$\Delta l$ (mm)	$\Delta l/l_m$ (%)	$T$ (h)
(1)	11.89	0.20	0.303	0.069	23	2.54
(2)	11.10	0.25	0.414	0.159	38	4.75
(3)	8.65	0.385	0.730	0.313	43	17

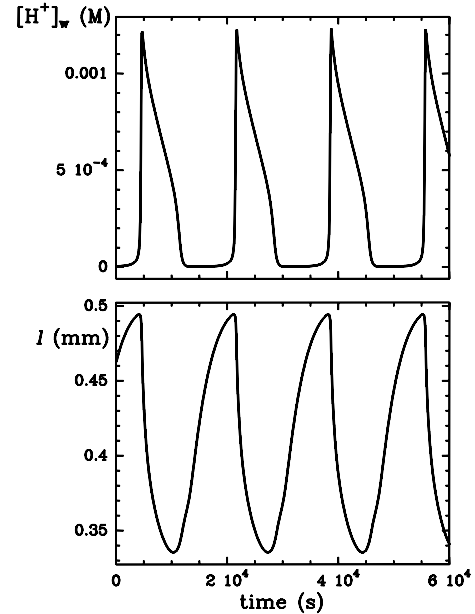


**Fig. 4.** Oscillations of size  $l$  and of  $[H^+]_w$  at the fixed wall for point (2) in Figure 3.  $[BrO_3^-]_0 = 25 \text{ mM}$ ,  $[SO_3^{2-}]_0 = 60 \text{ mM}$ ,  $[H_2SO_4]_0 = 11.10 \text{ mM}$ .  $l_0 = 0.25 \text{ mm}$ ,  $D_0 = 0.03 \text{ mm}^2/\text{s}$ ,  $\eta = 5$ .

points) is represented as vertical bars. In reference to the heuristic approach, the limits of spatial bistability already computed in Section 4 for the same parameters are also replicated from Figure 1. One must be aware that they are given for information but that they should be considered with caution. They were obtained for a stationary system and a fixed value of  $[HA]_0$ . In the present situation, the polymer volume fraction is not uniform. It has some influence on the diffusive transport, on the distribution of charges and additional convective motions are present. Moreover, the swelling time is not infinite in regard to the reaction/diffusion characteristic time. However, one can see that the minima and maxima of size during an oscillation are close to the bistability limits, in agreement with the heuristic theory.

As expected, the oscillations are periodic. The period  $T$  and the amplitude  $\Delta l$  of oscillations, for the three representative points in Figure 3 are reported in Table 3. To get a better idea of the effective size of the system, we have added  $l_m$ , the median value between the maxima and minima and the relative amplitude  $\Delta l/l_m$  (expressed in percent). For illustration, both the oscillations of size and

those of the concentration  $[H^+]$  at the fixed wall are shown in Figure 4 for point (2). Coupling the gel and the reaction not only induces mechanical pulsations but also gives rise to large  $pH$  oscillations in the deep core of the gel, whereas the CSTR/gel interface keeps fixed concentrations.

When the size increases, the period changes from a few hours to several days, so that using sizes  $l_m > 1$  mm would not be realistic from an experimental point of view. Close to the limits of the bistability region in a nonresponsive gel, *i.e.* at the largest  $[H_2SO_4]_0$  values (see point (1)) for which oscillations are observed, the amplitude of oscillations decreases as does the concentration gap between the two states. In this region, whereas the swelling time decreases with the system size, reaction dynamics exhibit some slowing down at the approach of the critical point so that the two characteristic times are getting closer and the oscillations present less relaxational features as can be seen in Figure 5 where we compare the shape of an oscillation at point (1) to the shape of an oscillation at point (3).

## 6 Discussion and conclusions

Although our analysis is applied to a 1-D system, one expects that qualitative behavior and orders of magnitude should be similar in other geometries since the increase in size ratio that could result from constraining the system to swell in a particular direction is somewhat counterbalanced by a larger shear stress that reinforces the elastic forces which limit swelling. Actually, preliminary experiments performed in our laboratory in conical gels evidence mechanical oscillations with a period of a few hours [51]. More elaborate experimental systems are presently developed to get confirmation and reliable data for a more systematic analysis. Examination of Figure 3 provides important information for experimentalists. An important result is that, for  $[H_2SO_4]_0$  lower than a value close to the critical bistability limit, there is *always* a small range of sizes in which the gel exhibits mechanical oscillations. Another point is that, even close to the critical bistability limit where small sizes allow for the shortest periods, the most suitable for experiments, the relative amplitude of oscillations remains large enough for observations.

Although the model seems able to provide good qualitative predictions and general trends, there are some important limitations and approximation levels that should be considered in the future. To conclude, let us briefly summarize the most important assumptions that could limit the validity of the model or its extensions to other problems. We have neglected the role of electrostatic interactions within the polymer chains. Their role is controversial, although most authors consider the entropic effect of the excess of free charges to be dominant. However, for strong densities of charges, counterions condensation [52] could significantly modify swelling predictions. We have, as usual, also replaced activities by concentrations but the domain of validity of this approximation is smaller for ionic solutions than for neutral species. We

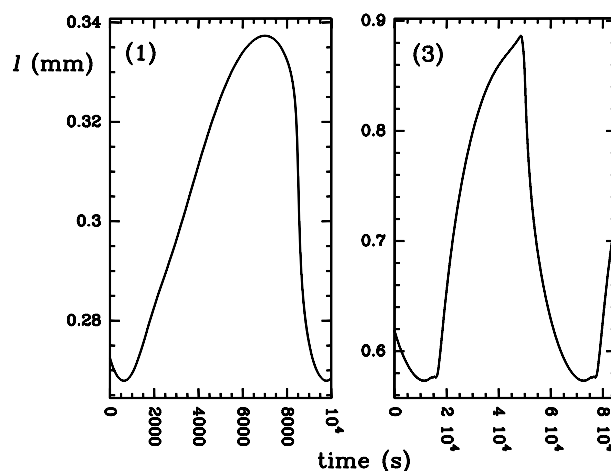


Fig. 5. Oscillation shapes for points (1) and (3) in Figure 3.

also assumed that the solutes are convected as the solvent and that their diffusion is only modified by steric hindrance by means of equation (30), neglecting all cross terms that would express other molecular interactions. By using a local Donnan equilibrium at the CSTR/gel boundary, we also implicitly assumed that the equilibria of the type  $H^+ + S^- \rightleftharpoons HS$  are much faster than other reactive processes. This means that in the stationary state of the CSTR, these reactions are actually at equilibrium, whereas these other processes only realize a collective balance. This is actually quite reasonable in the present case but could be questioned for other chemical systems. A more serious point is raised by the expression for  $\Pi_{ion}$  inside the gel given by equation (16) since the constant  $K_{ion}$  has to be set by reference to the values at the boundary. In a 1-D system with a CSTR at stationary state, the boundary condition is really invariant during the whole computation. Moreover, the value of this constant was found to present only small variations when the composition of the CSTR was changed within the flow state domain. Nevertheless, extension of the algorithm to nonstationary boundary conditions would need to reconsider this question. Finally, our approach is limited to the case of continuous size changes, which excludes a discontinuous volume transition. The dynamics of such transitions has only been considered on simple models with no charge, no ionic pressure and no chemical reaction [33]. At the present time, extension to such a situation is still out of reach, since, not only the dynamics of steep fronts would have to be accounted for, but the volume fraction of the polymer would be very large in the shrunken phase so that standard descriptions of transport would break down.

This work has been supported by CNRS and the Agence Nationale de la Recherche. I am indebted to I. Szalai and P. De Kepper for numerous discussions on the experimental developments and communication of their most recent results.

## References

1. I.R. Epstein, J.A. Pojman (Editors), *Nonlinear Dynamics Related to Polymeric Systems*, *Chaos* **9** (1999) (focus issue).
2. N.A. Peppas, P. Bures, W. Leobandund, H. Ichikawa, *Eur. J. Pharm. Biopharm* **50**, 27 (2000).
3. J.A. Pojman, Q. Tran-Cong-Miyata (Editors), *Nonlinear Dynamics in Polymeric Systems*, *ACS Symposium Series* **869** (ACS, Washington, 2003) p. 80.
4. P. Calvert, *MRS Bull.* **33**, 207 (2008).
5. P. Borckmans, P. De Kepper, A. Kholkhov, S. Métens (Editors), *Chemomechanical Instabilities in Responsive Material* (Springer, 2009) to appear.
6. R. Yoshida, T. Yamaguchi, H. Ichijo, *Mater. Sci. Eng. C* **4**, 107 (1996).
7. C.J. Crook, A. Smith, R.A.L. Jones, J. Ryan, *Phys. Chem. Chem. Phys.* **4**, 1367 (2002).
8. S. Villain, PhD Thesis, Univ. Paris VII (2007).
9. S. Villain, P. Borckmans, S. Métens, in ref. [5].
10. R. Yoshida, T. Takahashi, *J. Am. Chem. Soc.* **118**, 5134 (1996).
11. R. Yoshida, E. Kokufuta, T. Yamaguchi, *Chaos* **9**, 260 (1999).
12. R. Yoshida, M. Tanaka, S. Onodera, T. Yamaguchi, E. Kokufuta, *J. Phys. Chem. A* **104**, 7549 (2000).
13. V.V. Yashin, A.C. Balasz, *Macromolecules* **39**, 2024 (2006).
14. A.P. Dhanarajan, G.P. Misra, R.A. Siegel, *J. Phys. Chem. A* **106**, 8835 (2002).
15. G.P. Misra, R.A. Siegel, *J. Controlled Release* **81**, 1 (2002).
16. X. Zou, R.A. Siegel, *J. Chem. Phys.* **110**, 2267 (1999).
17. J. Boissonade, *Phys. Rev. Lett.* **90**, 188302 (2003).
18. J. Boissonade, *Chaos* **15**, 023703 (2005).
19. J. Boissonade, P. De Kepper, in ref. [5].
20. F. Gauffre, V. Labrot, J. Boissonade, P. De Kepper, in ref. [3].
21. V. Labrot, PhD Thesis, Univ. Bordeaux (2004).
22. V. Labrot, P. De Kepper, J. Boissonade, I. Szalai, F. Gauffre, *J. Phys. Chem. B* **109**, 21476 (2005).
23. J. Boissonade, P. De Kepper, F. Gauffre, I. Szalai, *Chaos* **16**, 037110 (2006).
24. T.G. Szántó, G. Rábai, *J. Phys. Chem. A* **109**, 5398 (2005).
25. Z. Virányi, I. Szalai, J. Boissonade, P. De Kepper, *J. Phys. Chem. A* **111**, 8090 (2005).
26. K. Benyaich, T. Erneux, S. Métens, S. Villain, P. Borckmans, *Chaos* **16**, 037100 (2006).
27. I.R. Epstein, J.A. Pojman, *An Introduction to Nonlinear Chemical Dynamics* (Oxford University Press, New York, Oxford, 1998).
28. P. Blanchedeau, J. Boissonade, P. De Kepper, *Physica D* **147**, 283 (2000).
29. M. Fuentes, M.N. Kuperman, J. Boissonade, E. Dulos, F. Gauffre, P. De Kepper, *Phys. Rev. E* **66**, 056205 (2002).
30. I. Szalai, P. De Kepper, *Phys. Chem. Chem. Phys.* **8**, 1105 (2006).
31. T. Tanaka, D.J. Fillmore, *J. Chem. Phys.* **70**, 1214 (1979).
32. A. Onuki, *Adv. Polym. Sci.* **109**, 63 (1993).
33. T. Tomari, M. Doi, *Macromolecules* **28**, 8334 (1995).
34. M.A.T. Bisschops, K.Ch.A.M. Luyben, L.A.M. van der Wielen, *Ind. Eng. Chem. Res.* **37**, 3312 (1998).
35. B. Barrière, L. Leibler, *J. Polym. Sci.* **41**, 166 (2003).
36. T. Yamaue, T. Taniguchi, M. Doi, *Mol. Phys.* **102**, 167 (2004).
37. T. Yamaue, M. Doi, *Phys. Rev. E* **69**, 041402 (2004).
38. P.J. Flory, *Principles of Polymer Chemistry* (Cornell University Press, Ithaca, 1953).
39. J. Rička, T. Tanaka, *Macromolecules* **17**, 2916 (1984).
40. U.P. Schröder, W. Oppermann, in *Physical Properties of Polymeric Gels*, edited by J.P. Cohen Addad (Wiley, Chichester, 1996) p. 19.
41. E.C. Achilleos, K.N. Christodoulou, I.G. Kevrekidis, *J. Comput. Polym. Sci.* **11**, 63 (2001).
42. J. Dolbow, E. Fried, H. Ji, *J. Mech. Phys. Solids* **52**, 51 (2004).
43. A.G. Ogston, B.N. Preston, J.D. Wells, *Proc. R. Soc. London, Ser. A* **333**, 297 (1973).
44. M. Doi, *Introduction to Polymer Physics* (Clarendon Press-Oxford University Press, Oxford, 1996).
45. A.Y. Grossberg, A.R. Kholkhlov, *Statistical Physics of Macromolecules* (AIP Press, New York, 1994).
46. J. Bastide, S.J. Candau, *Structure of gels investigated by static scattering techniques*, in *Physical Properties of Polymeric Gels*, edited by J.P. Cohen Addad (Wiley, Chichester, 1996) p. 143.
47. J. Newman, K.E. Thomas-Alyea, *Electrochemical Systems* (Wiley, New-York, 2004) Chapter 11.
48. E.M. Cussler, *Diffusion: Mass Transfer in Fluid Systems* (Cambridge University Press, Cambridge, 1997).
49. M.M. Tomadakis, S.V. Sotirchos, *AIChE J.* **39**, 397 (1993).
50. P. Kaps, P. Rentrop, *Numer. Math.* **33**, 55 (1979).
51. I. Szalai, P. De Kepper, private communication.
52. G. Manning, *J. Chem. Phys.* **51**, 924 (1969).